Süleyman Demirel Üniversitesi
Fen Bilimleri Enstitüsü Dergisi
Cilt 27, Sayı 1, 51-63, 2023

Süleyman Demirel University
Journal of Natural and Applied Sciences
Volume 27, Issue 1, 51-63, 2023

DOI: 10.19113/sdufenbed.1121167

Pharmacophore Modeling Guided by Conformational Dynamics Reveals Potent Anticancer Agents

Nigar KANTARCI-CARSIBASI*[1]

[1] Üsküdar University, Faculty of Engineering, Chemical Engineering Department, 34662, İstanbul, Turkey

(Alınış / Received: 25.05.2022, Kabul / Accepted: 07.11.2022, Online Yayınlanma / Published Online: 25.04.2023)

Keywords
elastic network model,
drug repurposing,
induced-fit docking,
MDM2,
p53

Abstract: Targeting the interaction between tumor suppressor p53 and murine double minute 2(MDM2) has been an attractive therapeutic strategy of recent cancer research. There are a few number of MDM2-targeted anticancer drug molecules undergoing clinical trials, yet none of them have been approved so far. In this study, a new approach is employed in which dynamics of MDM2 obtained by elastic network models are used as a guide in the generation of the ligand-based pharmacophore model prior to virtual screening. Hit molecules exhibiting high affinity to MDM2 were captured and tested by rigid and induced-fit molecular docking. The knowledge of the binding mechanism was used while creating the induced-fit docking criteria. Application of Molecular Mechanics-Generalized Born Surface Area (MM-GBSA) method provided an accurate prediction of the binding free energy values. Two leading hit molecules which have shown better docking scores, binding free energy values and drug-like molecular properties were identified. These hits exhibited extra intermolecular interactions with MDM2, indicating a stable complex formation and hence would be further tested in vitro. Finally, the combined computational strategy employed in this study can be a promising tool in drug design for the discovery of potential new hits.

Konformasyonel Dinamik Yönlendirmeli Farmakofor Modelleme ile Güçlü Antikanser Ajanlarının Belirlenmesi

Anahtar Kelimeler
elastik ağ modeli,
ilaç yeniden konumlandırma,
uyarılmış-uyumlu moleküler yerleştirme,
MDM2,
p53

Öz: Tümör baskılayıcı p53 ile Murine Double Minute 2 (MDM2) proteinleri arasındaki etkileşimi hedeflemek, son kanser araştırmalarında öne çıkan bir terapötik strateji olmuştur. Şu anda klinik deneylerde çalışılan birkaç MDM2 hedefli antikanser ilaç molekülü bulunmakla beraber hiçbiri henüz onay alamamıştır. Bu çalışmada, elastik ağ modelleri ile elde edilen MDM2 dinamiklerinin, ligand bazlı farmakofor modelinin oluşturulmasında ardından sanal tarama yürütülerek yeni MDM2 inhibitörlerinin araştırılmasında kılavuz olarak kullanıldığı bir yaklaşım yürütülmüştür. Sanal tarama sonucu elde edilen öncü moleküllerin MDM2'ye afiniteleri sabit ve uyarılmış-uyumlu moleküler yerleştirme (induced-fit docking) metodları ile test edilmiştir. İndüklenmiş yerleştirme kriterleri oluşturulurken bağlanma mekanizması bilgisi kullanılmıştır. Bağlanma serbest enerji değerlerinin doğru tahminini sağlayan Moleküler Mekanik Generalized Born-Surface Area (MM-GBSA) yönteminin uygulanması ile, yüksek yerleştirme puanları, bağlanma serbest enerjileri ve ilaca benzer fizikokimyasal özelliklere sahip iki adet lider molekül belirlenmiştir. Bu lider moleküller, MDM2 ile ekstra etkileşimler sergilerken kararlı kompleks oluşturmaktadırlar ve sonraki aşamada *in vitro* çalışmalarda incelenecekleridir. Sonuç olarak, burada uygulanan kombine bilgisayar destekli strateji, yeni ilaç adaylarının keşfinde başarılı bir yöntem olarak uygulanabilir.

**corresponding author: nigar.carsibasi@uskudar.edu.tr*

1. Introduction

Cancer is one of the most life-threatening health problems that corresponds to one-fifth death of all diseases worldwide and ranks second in death cases after cardiovascular disorders [1, 2]. Currently, cancer treatment involves chemotherapy in combination with radiation treatment and/or surgical removal. However, the existing anticancer drugs affect the normal cells as well as the cancer cells. As a result, serious side effects such as myelosuppresion, mucositis, hair loss, cardiotoxicity, neurotoxicity, and immunosuppression are encountered. Moreover, the cancer cells can undergo mutations in this way they may develop resistance to the available drugs. Therefore, to overcome both the existing problems of chemotherapy and to improve the patient's quality of life, anticancer agents that will be specifically cytotoxic towards the cancer cells only, with less side effects guide the recent cancer research [3]. Recently, chemotherapeutic agents consist of antimetabolites, DNA-interactive agents, anti-tubulin agents, hormones, and molecular targeting agents [4]. Tumor suppressor protein p53, has become one of the most important drug targets for cancer treatment since almost in all cancers, mutation or improper functioning of p53 has been detected [5]. P53 is a transcriptional factor that acts as the "guardian of genome" by playing crucial role in DNA repair and cell cycle arrest to prevent early cancerogenic events. When this repairing machinery fails, p53 induces apoptosis in the damaged cells, acting as a critical anti-cancer agent [6, 7]. In normal cells, p53 is kept at low levels by murine double minute 2 protein (MDM2) which binds to p53 transactivation domain and thus prevents its DNA binding ability, targets p53 to nuclear export or directly ubiquitinates p53 leading to its degradation [8, 9]. Consequently, blocking MDM2-p53 interaction by MDM2 antagonists has been an attractive therapeutic strategy of recent cancer research aiming to restore p53 function.

Despite the successful achievements obtained in clinical trial phases, still the need for less toxic, more specific and more potent drug candidates targeting MDM2 inhibition with less side effects is getting serious. At present there are several drug candidates as MDM2 antagonists undergoing clinical trials, namely: nutlins [10], RG7112 [11], RG7388 [12], SAR405838 [13], AMG-232 [14], NVP-CGM097 [15] and NVP-HDM201 [16] for which the details are provided in Table 1. Having limited number of molecules in clinical trials and the fact that none of them yet being FDA approved orients many works towards finding new inhibitors targeting MDM2 in order to boost p53 levels. Bringing a new drug into market is a challenging and expensive process, which requires an average of 10-15 years, an investment cost of about 1-3 billion dollars, though unfortunately the success rates are around 2% [17-19]. Due to these facts, computer aided drug design (CADD) strategies step out to be efficient, fast and powerful tools that would increase the success rates and reduce the cost and time requirements considerably.

Exploring protein dynamics by the investigation of conformational transitions bridges the gap between structure and function, which is crucial to understand the function of the protein and related binding mechanisms. Unfortunately, investigating protein-protein interactions and inhibition mechanism at the experimental level or with atomistic computational methods such as molecular dynamics is challenging, time consuming and requires high computational efficiency [20-22]. At this respect, Elastic Network Models (ENM), namely Gaussian Network Model (GNM) [23, 24] and Anisotropic Network Model (ANM) [25] prove successful to shed light on protein-protein or protein-small molecule interactions and binding mechanisms. Pharmacophore modeling in combination with virtual screening and molecular docking is a powerful strategy for discovery of novel compounds against a specific target. Many successful research have been put forth recently in this respect [26-32]. Ligand-based virtual screening methods enable fast screening based on a pharmacophore model that may be built upon a set of active ligands. Novel small molecule inhibitor design is likely to be a high costly and time-consuming process until the drug is approved and reaches the market. Therefore, generating a pharmacophore model based on the active available ligands undergoing clinical trials and validating the model by the conformational dynamics background to screen libraries can be a promising tool for potential new hits. There have also been several studies in which molecular docking, virtual screening and molecular dynamics tools were employed for the discovery of potent MDM2 inhibitors [33-41]. Some studies are conducted for elucidating the mechanism of binding of the native substrate p53 to MDM2. It was reported that an induced-fit mechanism was favored. Initially, p53 docks to the binding cleft of MDM2 and partially opens the binding site. Partial binding of p53 induces MDM2 to undergo conformational rearrangements aiming to further enlarge the pocket. Finally, p53 nicely fits into the binding pocket by maintaining interactions for a stable complex formation [42, 43].

Recently the conformational transitions and global motions of MDM2 and alterations brought about by the existence of its native inhibitor p53 and other small molecule inhibitors undergoing clinical trials were explored, using high efficiency low resolution elastic network modeling technique [44]. The aim of the present study is developing a new approach in the generation of the pharmacophore model prior to virtual screening in search for novel MDM2 inhibitors. Using these recent findings, a simulation strategy is conducted by incorporating protein dynamics in the generation and validation of the pharmacophore model. Virtual screening, rigid and induced-fit

molecular docking were carried out to capture several hit molecules showing high affinity to MDM2. The knowledge of the binding mechanism obtained from ENM was used while creating the induced-fit docking criteria. Molecular mechanics-generalized born surface area (MM-GBSA) method was utilized for more accurate prediction of the binding free energy. Moreover, insights about the binding mechanism served as a useful guide for the conduction of the induced-fit docking which can fine tune the docking strategy. Two hit molecules exhibiting extra interactions with the target with promising docking scores, binding free energy values and drug-like properties were proposed.

2. Material and Method

2.1. Protein Preparation

The crystal structures of MDM2 complexed with small molecule inhibitor complex systems are obtained from the Protein Data Bank and prepared using Schrödinger's Maestro Molecular Modeling Suite [45, 46] and protein preparation wizard module [47]. Among the available MDM2 protein structures as listed in Table 1, the lowest RMSD value between the co-crystal ligand and the best re-docked pose was attained in the case of 5OC8 as also discussed in recent previous work [44]. So the MDM2 of 5OC8 pdb-coded structure was used in all docking calculations as macromolecular target. Target protein is first corrected for bond orders and missing hydrogen atoms. All heteroatoms other than the native ligand are removed. But the water atoms within 5 Å around the binding cleft were kept. In case there are any missing side chains or missing loops, Prime module was used to fill in these gaps (though this structure did not have any). Protonation states were generated using PROPKA at pH: 7.0. Finally, restrained minimization was carried out using 0.3 Å RMSD and OPLS2005 (Optimized potentials for liquid simulations 2005) force field [48].

2.2. Ligand Preparation

Prior to all docking simulations, the ligands were prepared using LigPrep module of Maestro, Schrödinger software [46, 47]. Ionization states and tautomers were generated using Epik at pH: 7.0 ± 2.0 [49]. Stereoisomers were generated using chiralities from the 3D structure of the ligands.

2.3. Pharmacophore Model Generation

A 3-D pharmacophore model is a set of chemical features or functionalities aligned in three dimensional space. The essential interactions of small molecule ligands with the receptor binding site can then be represented via this spatial arrangement of chemical features. The pharmacophore model represents the chemical properties and 3D structure of a ligand, using one of the interaction types to form hydrogen bonding, hydrophobic, electrostatic, and charge transfer interactions [50, 51]. In this context, LigandScout 4.4.7 simulation program [51] was used to construct a pharmacophore model based on 7 X-ray crystal structures of human MDM2 inhibitors that are undergoing clinical trials as the relevant details such as protein data bank code (pdb code), half-inhibitory concentration (IC_{50}), crystal structure resolution (Res.) and the related references (Ref.) are provided in Table 1.

Separate structure-based pharmacophore models were generated using Ligand Scout 4.4.7 based on the crystal structures of these 7 inhibitors. X-ray structures were downloaded from Protein Data Bank automatically by Ligand Scout 4.4.7. The ligands were explored in detail in ligand-based perspective and energy minimized by MMFF94 force field [52] in order to generate possible minimum energy states. Initially, separate pharmacophores were generated from the interaction of these ligands with MDM2 receptor using pharmacophore generation tool in LigandScout 4.4.7. Then all seven pharmacophore hypotheses were aligned onto the reference pharmacophore of the reference receptor structure (pdb code: 5OC8) to extract the shared features using the shared feature generation module. Finally, the exclusion volumes were added to finalize the pharmacophore model for 3D query in virtual screening.

Table 1. Several MDM2 inhibitors undergoing clinical trials

Molecule	Pdb Code	IC_{50} (nM)	Res. (Å)	Ref.
Nutlin3	4J3E	90	1.9	10
RG 7112	4IPF	18	1.7	11
RG 7388	4JRG	6	1.9	12
SAR405838	5TRF	0.88	2.1	13
AMG 232	4OAS	0.6	1.7	14
NVP-CGM097	4ZYI	1.7	1.67	15
NVP-HDM201	5OC8	0.21	1.56	16

2.4. Molecular Docking (Rigid Docking and Induced Fit Docking Protocols)

Molecular docking is a fast and powerful tool to find the best conformation among the possible ones that would fit the binding site of the receptor. Minimum energy conformation with maximum possible interactions is of interest. Molecular docking can supply a relative comparison of the binding affinities and thus potencies of available drug molecules towards target protein. The more negative the binding affinity value is, the more strongly the molecule interacts with the receptor. The protein of interest MDM2 is a structurally disordered and highly flexible protein which gain stability upon binding. This phenomena points out to the induced fit mechanism of MDM2 upon binding to inhibitors. Hence rigid docking

strategies may mislead while performing molecular docking with MDM2. Both strategies were performed and the results were compared.

2.4.1. Rigid docking

Once the common feature pharmacophore model was generated the Drug Bank [53] library of 9067 molecules with known 3D structures was screened. The hits which match the pharmacophore (2177 hit molecules) were retrieved and then Lipinski's Rule of five [54] and polar surface area pre-filters (polar surface area is preferred to be ≤ 140 Å) were applied and the remaining molecules (267 molecules) were first docked using Autodock Vina [55] which is incorporated within Ligand Scout software. Default parameters were used with the number of conformations generated being 9, exhaustiveness value of 3 and the maximum energy difference being 3. Molecules having considerably high docking scores (≤ -8.5) kcal/mol were further docked using Glide SP (standard precision) and XP (extra precision) algorithms [56, 57] in Ligand Docking Module of Schrödinger Suite. The grid box was generated for the target MDM2 around the binding cleft centered on the centroid of the co-crystal ligand NVP-HDM201 (pdb code: 5OC8) using the Receptor Grid Generation module. Size of the grid box was selected to enable docking of the ligands with length ≤ 20 Å. Same grid file was used in all docking simulations for a reliable comparison. All the docked ligands were prepared by LigPrep module prior to docking as explained above. Ligands were kept flexible and Epik state penalties were added to docking scores. Maximum of ten poses were obtained for each ligand.

2.4.2. Induced Fit Docking (IFD)

Ligands that were prepared by LigPrep module of Schrödinger and all possible conformers for each ligand were docked to protein binding site with the same grid file prepared for rigid docking this time by accounting the protein flexibility. IFD generates binding poses for targets by considering both ligand and receptor conformational flexibility, which is crucial for more accurate docking of the ligand. IFD protocol [58] uses Glide to sample ligand binding modes and Prime to sample protein flexibility. Glide/SP docking was employed by changing the grid size to allow ligands ≤ 20 Å size to be docked, similar to rigid SP/XP docking protocols described above. By default, the ligand and the side chain residues within 5 Å were refined and optimized. Receptor and ligand Van der Waals scaling factors were 0.7 and 0.5 by default. IFD protocol uses side-chain trimming option in order to create more room in the active site so that the non-native ligand can be sampled thoroughly. The importance of helix-4 and basically Tyr 100 residue located in this region was illuminated in previous work. The size of the binding cleft was shown to be mainly controlled by the modifications in helix-4 region. This region, outshined by Tyr 100 mainly, acts as a gate keeper, by keeping the cleft closed in the unbound; and open in bound states for better penetration and docking of the ligands. Hence Tyr 100 residue side chain which is in close proximity with the ligand to be docked was trimmed while conducting IFD protocol so as to prevent any hindering effect. This residue was temporarily mutated to Alanine during the initial Glide docking, and then converted back during redocking by Glide after the side chain residues within 5 Å were optimized and refined by Prime module. Each ligand was finally redocked with Glide/SP and 20 poses were obtained.

2.5. Conformational Dynamics and Mode Shapes by Elastic Network Models GNM and ANM

GNM is a fast and efficient analytical approach that can be used for bridging the gap between global motions and biological functions of proteins. The vibrational dynamics of the protein is modeled by placing a node to each alpha-carbon of residues and connecting them with springs. Harmonic potential of the system and residue mean-square fluctutations are calculated. Total residue fluctuations are decomposed into high and low frequency fluctuations, namely fast and slow (or soft) modes [23, 24]. The fast modes, i.e. the high frequency fluctuations, correspond to the kinetically hot residues (binding hot spots) while the slow modes are associated with global (collective) dynamics of the overall structure. In the previous work [44] by using GNM and ANM, the global dynamics of MDM2 and the conformational changes it undergoes upon ligand binding in cases of both native ligand p53 and small molecule inhibitors NVP-CGM097 and NVP-HDM201 binding were analyzed. Moreover, the domain motions in the softest modes were also illustrated around the binding site. Three distinct conserved regions were identified in MDM2 namely, Regions I (residues 50-77) and III (residues 90-105) corresponding to the binding interface of MDM2 including α helix-2 (α2), Loop-2 (L2), and α helix-4 (α4) domains which were actually stabilized during complex formation. Region II (residues 77-90), exhibiting high amplitude collective motion, was a highly flexible region in both unbound and complex forms. In the light of these findings, the pharmacophore was validated and made sure that the essential three distinct regions of MDM2 were comprised.

2.6. Molecular Mechanics, the Generalized Born Model and Solvent Accessibility (MM-GBSA)

Docking scores may only give a relative comparison between the compounds. A more thorough analysis on free energy of binding is carried out by MM-GBSA method. To perform more accurate binding free energy calculation, Prime MM-GBSA module of Schrödinger Suite was used. Free energy of binding can be expressed as the sum of the enthalpic and entropic contributions as follows:

$$\Delta G_{bind} = \Delta H - T\Delta S \quad (1)$$

Since similar types of ligands are docked to the receptor, the entropic contribution can be neglected and hence:

$$\Delta G_{bind} \cong \Delta H \quad (2)$$

Enthalpic contribution includes molecular mechanics energy (ΔE_{mm}) of the molecule and solvation energy (ΔG_{sol}). Further, molecular mechanics energy of the molecule can be expressed by sum of its internal energy, electrostatic and van der Waals interactions; while the solvation energy is composed of polar (ΔG_{GB}) and non-polar (ΔG_{SA}) contributions [59, 60]:

$$\Delta G_{bind} = \Delta E_{mm} + \Delta G_{sol} \quad (3)$$

$$\Delta E_{mm} = \Delta E_{internal} + \Delta E_{electrostatic} + \Delta E_{vdW} \quad (4)$$

$$\Delta G_{sol} = \Delta G_{GB} + \Delta G_{SA} \quad (5)$$

Resulting complexes obtained as a result of IFD calculations were processed by Prime-GBSA to obtain free energy of binding values. IFD simulations returns a set of complexes as an output with the corresponding IFD score, i.e. different poses are valid for the ligand as well as for the receptor. Since output file of IFD simulations contain different protein-ligand complex conformations, the complex with the highest IFD score was selected and splitted up into its protein and ligand to carry out the MM-GBSA calculation. The solvation model used was VSGB [61], force field was OPLS2005 [48], and protein flexibility was allowed within 5 Å distance from the ligand.

2.7. Virtual Screening Protocol and Workflow of the Methodology

Figure 1 depicts the workflow employed in the present study. Drug/drug-like compounds retrieved from Drug Bank with known 3-D structures were screened against a shared feature pharmacophore which was guided by elastic network modeling results. First filtering was applied according to the pharmacophore fit score and further filtering was applied according to Lipinski's rule of fives and polar surface area criteria. Predocking was accomplished by Autodock Vina and comparably strong binders are identified and docked using Glide SP/XP docking. Top ten highest docking score molecules were then processed with IFD where side chain trimming was employed for Tyr100 residue to enlarge the active site in the light of ENM results. For the top ten hit molecules more sophisticated free energy of binding analysis was conducted using MM-GBSA method that pointed out to leading hit molecules that may serve as promising MDM2 inhibitors which exhibit better binding as compared to the clinical trial compounds.

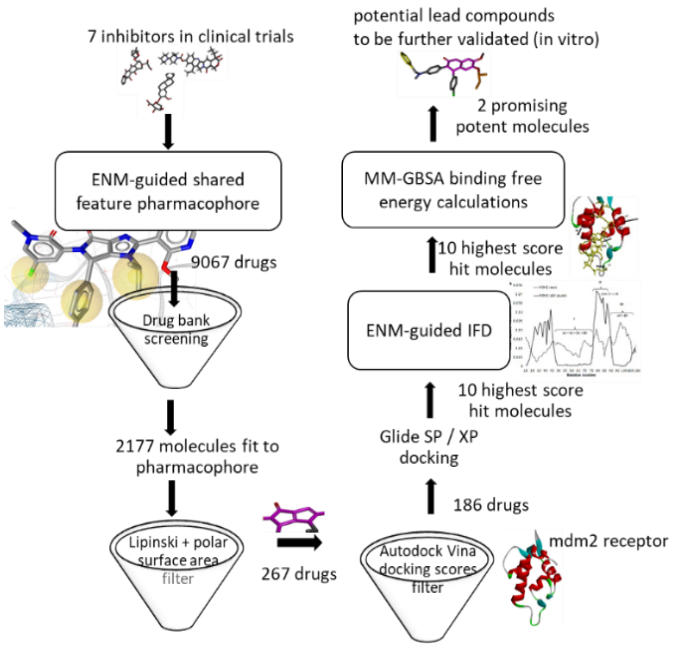

Figure 1. Schematic of the ENM-based pharmacophore model generation, virtual screening, docking and MM-GBSA calculation workflow

3. Results

3.1. ENM-guided Pharmacophore model generation and validation

The interaction of the most potent inhibitor under clinical trials NVP-HDM201 (pdb code: 5OC8) with the MDM2 active site is depicted in Figure 2.

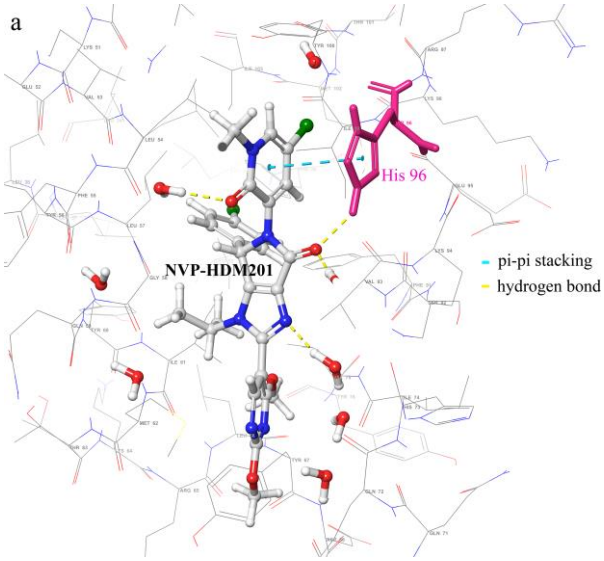

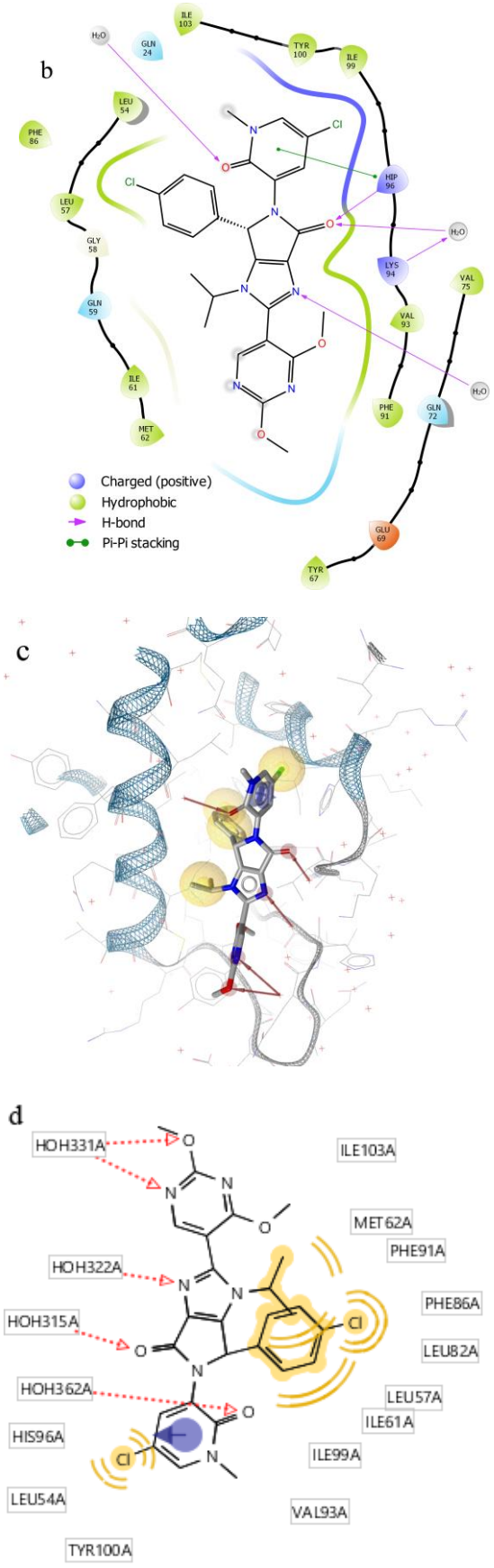

Figure 2. 3-D (a) and 2-D (b) binding site and interactions of NVP-HDM201 with MDM2 (pdb code: 5OC8). (c) 3-D Pharmacophore model of NVP-HDM201 (d) 2-D representation of the pharmacophoric features

The binding site interaction maps for 3-D and 2-D are demonstrated in panels a and b, respectively. The most crucial interaction is the hydrogen bonding accomplished between His 96 of MDM2 and pyrrolidine ring of the inhibitor (indicated in blue dashed line in panel a). Besides, there are hydrophobic interactions between Leu 54 and Leu 57 binding site of MDM2 with Cl attached pyridine group and Ile 99 and Tyr 100 binding site with chlorophenyl group of the ligand (panel b). The ligand also exhibits hydrogen bonding with surrounding water molecules (yellow dashed lines in panel a). The pharmacophore model generated with NVP-HDM201 is provided in panel c. The key pharmacophoric features are basically: 4 hydrophobic regions (yellow), 1 aromatic ring (blue) and 5 hydrogen bond acceptor groups (panel d red arrows).

In the light of previous work [44], it was elucidated that the protein can basically be separated into three distinct regions: Region I, II and III (Figure 3, panel a). Region I and III consist of active site residues that take role in binding and hence the flexibilities of these residues are hindered upon binding by the stabilizing interactions. These are the hinge regions of protein with restricted motion that are located in the minima of residue fluctuation profile. Region II serves as the most flexible region for which the flexibility is even enhanced in presence of inhibitors enabling the neighboring regions to participate in binding. So basically, it is evident that Region I and III should be accounted for while figuring
out the pharmacophore model to be used in virtual screening.

Regions I and III are comprised of the hydrophobic features (yellow spheres) for inhibitor NVP-HDM201 as presented in Figure 3, panel b. A pharmacophoric query was then generated using a shared feature model obtained from overlapping features of seven clinical trial inhibitor molecules listed in Table 1. A three feature pharmacophore model was obtained (Figure 3, panel c), consisting of three hydrophobic groups and utilized it in the virtual screening process. Indeed, the three hydrophobic features (yellow spheres) enclose the essential domains of MDM2 (regions I and III).

Before proceeding with the virtual screening, the model should be first validated. The model should successfully retrieve the active compounds from a database, i.e. differentiate between the actives and inactives (decoys). For this purpose a ROC (receiver operating characteristics) curve, which is a graphic representation of the relation existing between the sensibility and the specificity of a test, is plotted. Fraction of true positive rate (TPR) out of the total actual positives are plotted against the fraction of false positive rate (FPR) out of the total actual negatives. TPR (sensitivity) and FPR (specificity) are stated as follows:

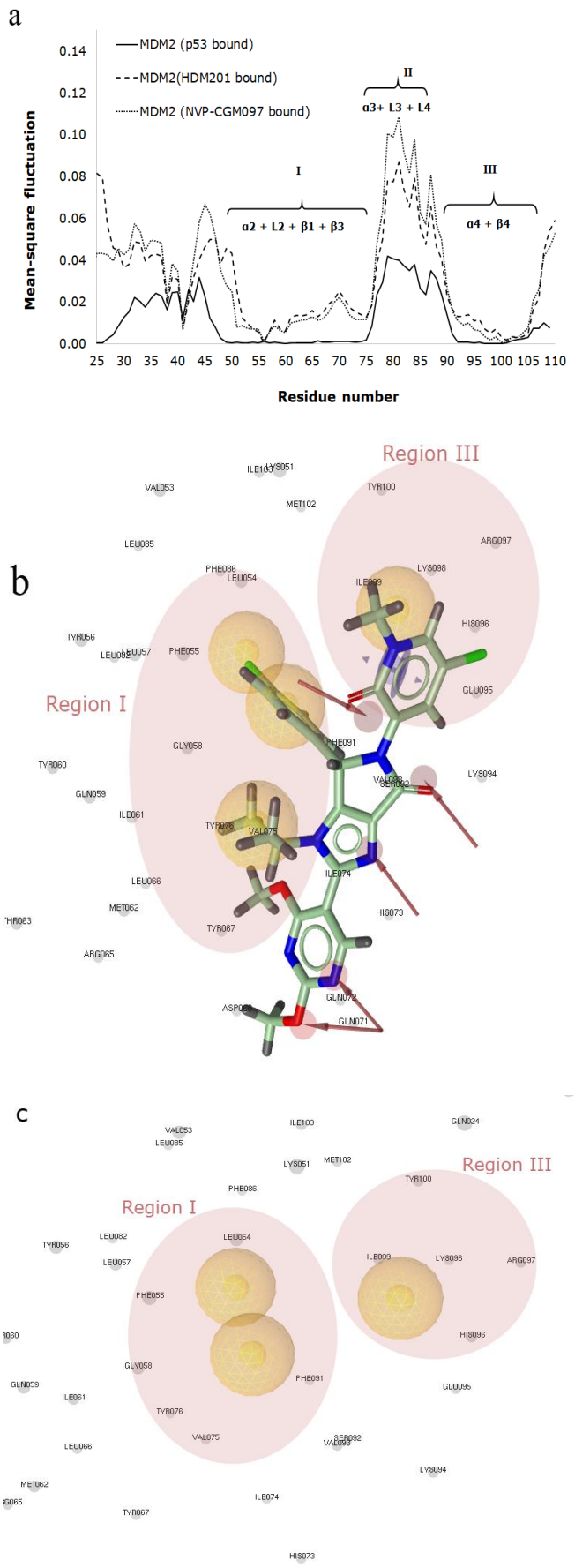

Figure 3. Pharmacophoric features overlapping with the essential hinge regions (Regions I and III) in MDM2 (a) Mean-square fluctuations of MDM2 in the presence of inhibitors (b) Pharmacophore model generated with NVP-HDM-201 inhibitor consisting of 4 hydrophobic regions (yellow spheres) and 5 hydrogen bond acceptor groups (red arrows) (c) Shared feature pharmacophore used in virtual screening. Three features that are common in all seven inhibitors are the three hydrophobic regions overlapping with the essential binding regions (Region I and III).

$$TPR\ (sensitivity) = TP/(TP+FN) \quad (6)$$

$$FPR\ (specificity) = TN/(TN+FP) \quad (7)$$

where, TN and TP are true negative and true positive values; and FN and FP are false negative and false positive values respectively [62, 63]. In this case, we it will be used for checking whether the pharmacophore model based virtual screening is able to differentiate active ligands from the inactive ligands (decoys). The area under the curve (AUC) can also be used to test the efficiency of the method. An excellent model has AUC near 1 which means it has a good measure of separability. A poor model has an AUC near 0 which means it has the worst measure of separability [64]. The ROC curve is plotted using Ligand Scout virtual screening module, prior to screening (you may refer to Appendix A, Figure A.1.). The active set was prepared with 23 molecules obtained from literature for which the activity data exists for inhibition of MDM2. The decoy set was 9067 compounds (from DrugBank) with unknown activity against MDM2. The ROC plot indicated that AUC= 0.99 and Enrichment Factor (EF)= 22, which means that the model is rational and will be able to distinguish between positive class and negative class [29]. EF value of 22 means, we observe 22 times more active compounds in the top 1% of our results.

3.2. Virtual Screening and Capturing Hit Molecules

The Drug Bank [53] library of small molecules which consist of 9067 drug and drug-like compounds for which 3-D structure exists was screened and 2177 hits, which match the 3-feature pharmacophore model validated by statistical and ENM based models, were obtained. As a prefilter the ligands that do not obey Lipinski's Rule of Five were removed and also the value of the polar surface area is maintained to be less than or equal to 140 Å. The number of hits retrieved were 267 to be docked into MDM2 binding pocket. Pre-docking by Autodock Vina which was incorporated in the Ligand Scout 4.4.7 was employed. The grid box was generated based on the pdb structure of NVP-HDM201 (pdb code: 5OC8). Docking resulted in totally 2351 different conformations together with corresponding binding affinity values. The strong binders were retrieved with binding affinity values less than -8.5 kcal/mol. Top 10% of highest affinity molecules (~186 molecules) were then docked with Glide SP (standart precision) and XP (extra precision) which were rigid docking strategies as well. Both SP and XP relies on empirical scoring functions. Glide XP performs with a more extensive sampling as compared to SP and uses more sophisticated scoring function for prediction of

binding affinities [57]. Since MDM2 is shown to possess an induced-fit mechanism upon binding, top 10 good scoring molecules were then re-docked by using ENM-guided IFD protocol (induced fit docking) of Schrödinger. At the final stage, more thorough free energy of binding calculations were performed by MM-GBSA method which was processed by using IFD best scoring conformations. The ten hit compounds retrieved together with the corresponding docking scores and MM-GBSA binding free energy values are enlisted in Table 2 in comparison with the clinical trial inhibitors.

Table 2. Glide SP/XP/IFD docking scores and MM-GBSA binding free energy results of highest scoring 10 hit molecules

DrugBank ID	Brand name	Approved/ investigational	Glide-SP DScore (kcal/mol)	Glide-XP DScore (kcal/mol)	Induced-Fit DScore (kcal/mol)	MM-GBSA (kcal/ mol)
Clinical	NVP-HDM201 (Siremadlin)	Clinical trials for MDM2 inhibition	-11.1	-11.3	-12.4	-90.8
Clinical	NVP-CGM097	Clinical trials for MDM2 inhibition	-9.9	-10.1	-10.8	-83.5
Clinical	Nutlin3	Clinical trials for MDM2 inhibition	-8.9	-9.4	-10.2	-70.3
06666	Lixivaptan	Clinical trials for treatment hyponatremia and congestive heart failure	-9.0	-9.5	**-12.7**	**-94.3**
04016	not available	experimental	-11.0	-10.2	**-13.7**	**-86.0**
04852	Implitapide	Clinical trials for treatment of atherosclerosis	-8.9	-9.7	-10.1	-81.6
00637	Astemizole	Approved/ withdrawn for treatment of allergy symptoms	-8.7	-8.3	-9.3	-79.7
16266	Olodanrigan	Clinical trials for treatment of diabetic neuropathies	-8.5	-8.9	-9.8	-79.6
11399	Slentrol, dirlotapide	Approved for managing obesity in dogs (not for human use)	-9.5	-9.3	-9.9	-78.2
11787	Ralimetinib	Clinical trials for treatment of breast and ovarian cancer	-8.1	-7.6	-8.9	-72.5
02668	JE-2147 tigecycline	experimental	-8.3	-9.5	-12.1	-70.0
12457	Rimegepant	Approved for treatment of migraines	-8.8	-8.1	-8.4	-64.2
09280	Lumacaftor	Approved for treatment of cystic fibrosis	-7.3	-6.9	-7.7	-42.4

Most potent clinical trial molecules for MDM2 inhibition (NVP-HDM201, NVP-CGM097 and nutlin3) are given in the first three rows. Out of ten hits, two compounds (**DB 06666** and **DB 04016**) step forward in terms of better MM-GBSA and docking scores (values indicated in bold) as compared to potent clinical trial molecules. For sure, the more negative the values of MM-GBSA binding free energy and docking score, the stronger the compound would bind to the target. Hence compounds DB 06666 (lixivaptan) and DB 04016 are expected to have promising potencies as compared to the clinical trial compounds and deserves further experimental validation.

Pharmacophore model mapping together with 3-D and 2-D interactions of the two hit compounds (DB 06666 and DB 04016) are depicted in Figures 4 and 5, respectively. Investigation of the interactions accomplished by DB 06666 (lixivaptan) reveals that in addition to hydrogen bonding accomplished between His 96 of MDM2 and pyrrolidine ring of the inhibitor NVP-HDM201, lixivaptan exhibits additional interactions (Figure 4). His 96 of MDM2 makes hydrogen bonding with –NH group that lies between the chlorophenyl and fluorophenyl ring groups of lixivaptan. At the same time, pi-cation and pi-pi stacking interactions are also detected between His 96 and the chlorophenyl ring of lixivaptan. Other than His 96, Tyr 100 residue is inspected to participate in pi-pi stacking interaction with the fluorophenyl group of lixivaptan (Figure 4b and 4c). These interactions would have positive contributions to the total binding free energy and stability of lixivaptan in the binding site.

The crucial role of Tyr 100 in the active site interactions was previously discussed and mentioned in literature [37]. Its participation would enhance the stability of the complex which agrees with the findings obtained here. As a result, lixivaptan interacts with MDM2 through helix-4 residues, namely His 96 and Tyr 100. The mapping of the other leading hit compound DB 04016 onto the pharmacophore model together with the binding site interactions are depicted in Figure 5. Investigation of the interactions of compound DB 04016 with MDM2 revealed that His 96 participates in pi-pi stacking and pi-cation interactions, additionally, His 96 together with Lys 94 creates salt-bridges with DB 04016 (Figure 5b and 5c). Gln 72 and Leu 54 contribute to hydrogen bonding reaching the compound DB 04016, by the help of surrounding water molecules. Overall, DB 04016 interacts through all essential residues mentioned in literature, namely Gln 72, Leu 54, Lys 94 and His 96 that are known to contribute to the majority of the binding free energy in the active site.

3.3. Drug-likeness and molecular properties of the two leading hit compounds

Lixivaptan (DB 06666) belongs to the class of benzanilides, which are aromatic compounds containing an anilide group. It is investigated for use/treatment in hyponatremia and congestive heart failure (65, 66). DB 04016 is an experimental compound belonging to the class of organic compounds known as stilbenes. It is known to interact with Cathepsin G (Serine-type endopeptidase) found in human which has antibacterial activity; and with Chymase (Serine-type peptidase) again in human which is suspected to play roles in vasoactive peptide generation, extracellular matrix degradation, and regulation of gland secretion [65-67].

Several molecular descriptors (molecular weight, solubility, lipophilicity, topological polar surface area, plasma protein binding and human intestinal absorption) are tabulated for these two leading hit compounds and compared with two potent MDM2 inhibitors (Table 3). Values are obtained using AlogPS [68] and PreAdmet [69].The molecular property values of the two leading hit molecules are found to be in acceptable ranges for drug-likeness.

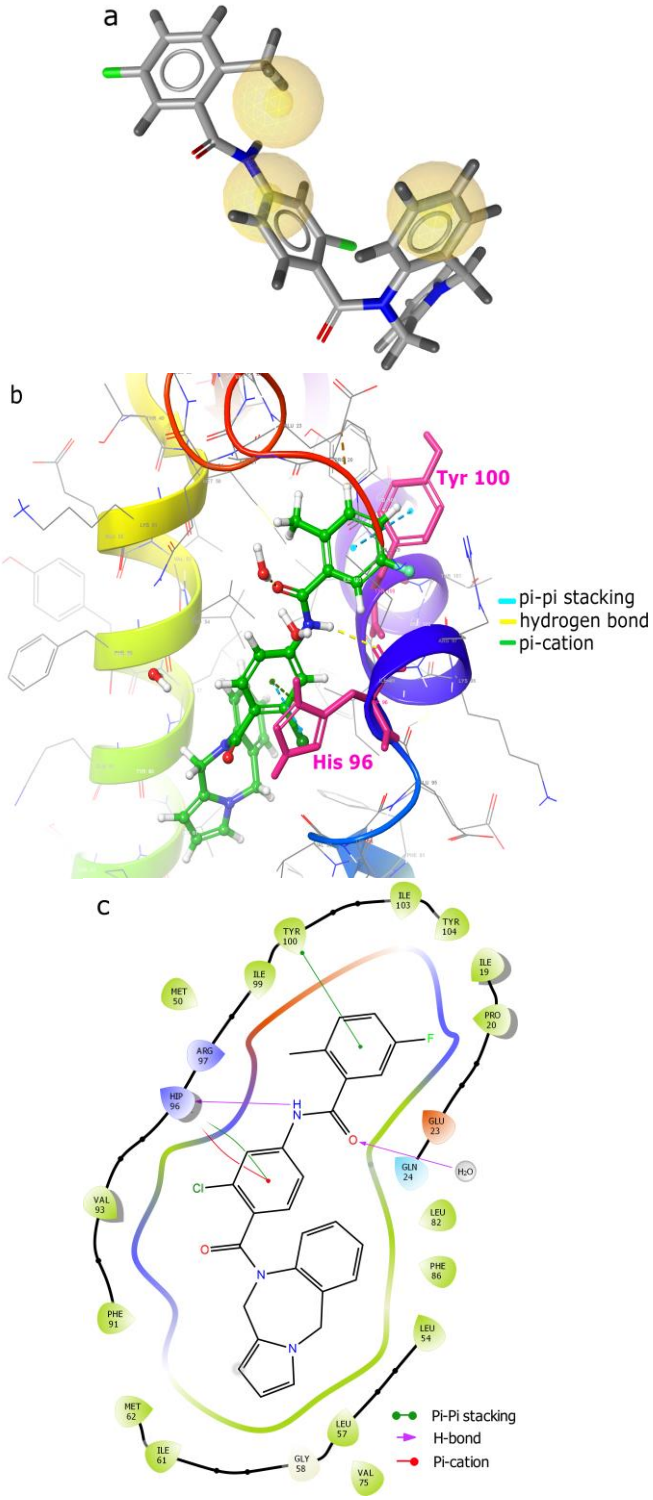

Figure 4. Pharmacophore model alignment (a), 3-D (b) and 2-D (c) interactions of the hit compound DB 06666 (lixivaptan) in the binding site

Table 3. Molecular properties of two potent MDM2 inhibitors and two leading hit compounds

Molecule	Mol.W. (g/mol)	Log S [a] (Alogps)	Log P [b] (Alogps)	TPSA [c] (Å)	P.prot.bind [d] (%)
NVP-CGM097	659.3	-5.3	6.6	65.6	88.0
NVP-HDM201	555.4	-4.8	4.19	102.68	92.3
DB 06666	473.9	-6	4.99	54.34	92.1
DB 04016	670.6	-6.7	4.49	115.22	100

[a] log S: pure water solubility (log S ≤ -6.0 insoluble; -4.0 ≤logS ≤-6.0 moderately soluble)
[b] log P: lipophilicity (suitable if ≤ 5)
[c] topological polar surface area (suitable if ≤ 140 Å^2)
[d] plasma protein binding (strong binder if ≥ 90%)
[e] human intestinal absorption (well absorbed if ≥ 70%)

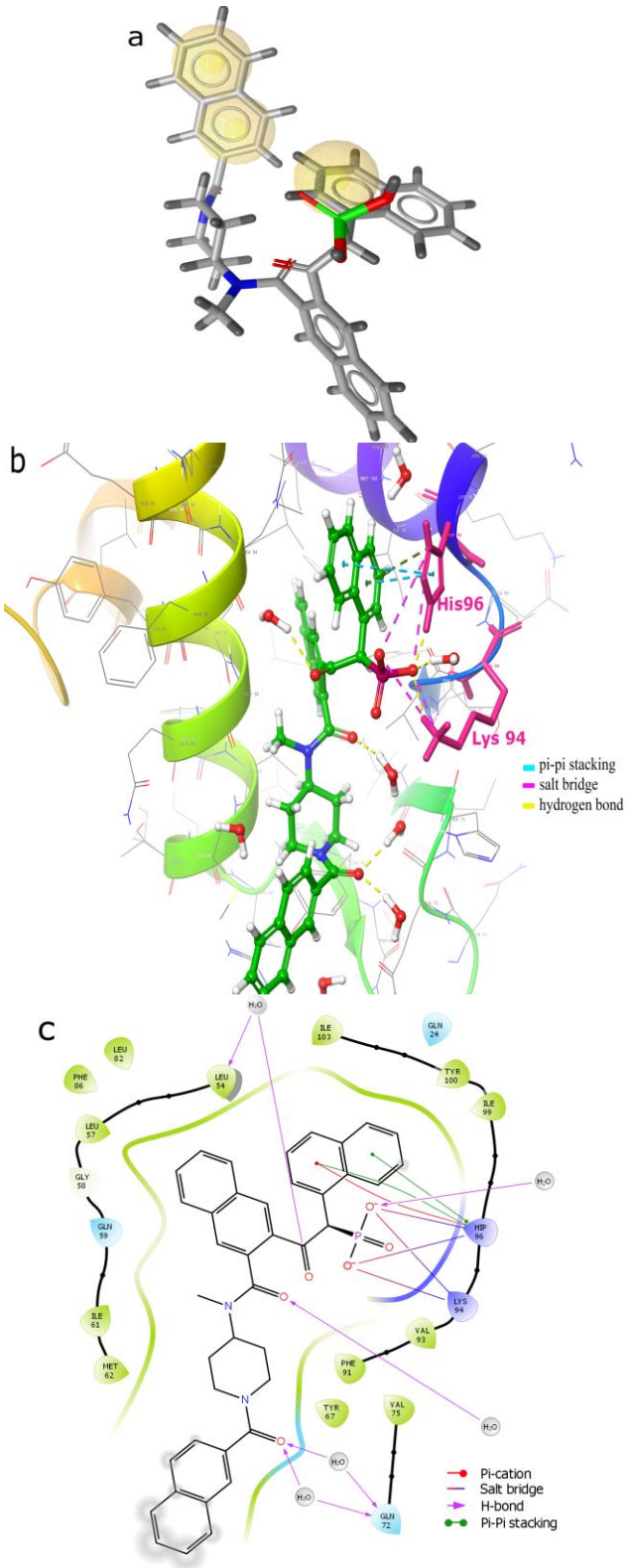

Figure 5. Pharmacophore model alignment (a), 3-D (b) and 2-D (c) interactions of the hit compound DB 04016 in the binding site

4. Discussion and Conclusion

The absence of an FDA-approved drug yet, inspires drug development studies to be targeted on the MDM2 protein. In this study, an ENM-guided pharmacophore model generation and validation based on shared features among the seven potent clinical trial MDM2 inhibitor molecules was presented. This model was then used to screen the Drug Bank database for which 3-D structures exist. Due to the intrinsically disordered dynamics of MDM2, induced-fit docking was preferred together with other docking methods in the filtration of database. The binding modes obtained from the ENM simulations were also used in the creation of the IFD protocol. Lipinski rule of five and polar surface area criterion were applied for the elimination. Advanced free energy of binding calculations by MM-GBSA scoring functions helped to identify top ranked hit molecules which have high affinity towards MDM2. MM-GBSA calculations performed over docking trajectory provided useful knowledge about binding free energies. Further studies may be conducted with Molecular Dynamics (MD) Simulations and MM-GBSA culculations may also be performed concerning MD trajectories. It was worth noting besides their high docking scores, the two leading hits obtained (DB 06666 and DB 04016) have extra intermolecular interactions with MDM2 which indicates a stable complex formation as compared to the clinical trial MDM2 inhibitors. Having molecular properties in suitable ranges contributes positively for the hit compounds to be drug-like and can be further tested by *in vitro* experiments. The combined computational strategy employed in this study may serve as a useful tool in the initial step of drug design or drug-repurposing which would contribute to saving time and money.

Acknowledegements

Helpful suggestions of Dr. Abdulillah Ece from Biruni University Pharmacy Department and technical supports of Rita Podzuna from Schrödinger Inc. are gratefully appreciated.

References

[1] Ferlay, J., Colombet, M., Soerjomataram, I. 2019. Estimating the global cancer incidence and mortality in 2018: Globocan sources and methods. International Journal of Cancer, 144 (8), 1941-1953.

[2] Siegel, R. L., Miller, K. D., Jemal, A. 2016. Cancer statistics. CA Cancer Journal for Clinicians 2016, 66, 7-30.

[3] Singh, S., Sharma, B., Kanwar, S., Kumar, A. 2016. Lead phytochemicals for anticancer drug development. Frontiers in Plant Science, 7, 1667.

[4] Choudri, A. S., Mandave, P. C., Deshpande, M., Ranjekar, P., Prakash, O. 2020. Phytochemicals in cancer treatment: From preclinical studies to clinical practice. Frontiers in Pharmacology, 10, 1614.

[5] Khoo, K. H., Verma, C. S., Lane, D. P. 2014. Drugging the p53 pathway: understanding the route to clinical efficacy. Nature Reviews Drug Discovery,13, 217-236.

[6] Lane, D. P. 1992. P53, guardian of the genome. Nature, 358, 15–16.

[7] Skalniak, L., Surmiak, E., Holak, T. A. 2019. A therapeutic patent overview of MDM2/X-targeted therapies (2014-2018). Expert Opinion on Therapeutic Patents, 29 (3), 151-170.

[8] Momand, J. G., Zambetti, P., Olson, D. C., Donna, G., George, D., Levine, A. J. 1992. The MDM2 oncogene product forms a complex with the p53 protein and inhibits p53 mediated transactivation. Cell, 69 (7), 1237-1245.

[9] Roth, J., Dobbelstein, M., Freedman, D., Shenk, T., Levine, A. J. 1998. Nucleo-cytoplasmic shuttling of the hdm2 oncoprotein regulates the levels of the p53 protein via a pathway used by the human immunodeficiency virus rev protein. Embo Journal, 17, 554-564.

[10] Vassilev, L. T., Vu, B. T., Graves, B., Carvajal, D., Podlaski, F. 2001. In vivo activation of the p53 pathway by small-molecule antagonists of MDM2. Science, 303, 844-8.

[11] Vu, B., Wovkulich, P., Pizzolato, G., Lovey, A., Ding, Q., Jiang, N. 2013. Discovery of RG7112: a small-molecule MDM2 inhibitor in clinical development. ACS Medicinal Chemistry Letters, 4, 466−9.

[12] Ding, Q., Zhang, Z., Liu, J. J., Jiang, N., Zhang, J., Ross, T. M. 2013. Discovery of RG7388, a potent and selective p53-MDM2 inhibitor in clinical development. Journal of Medicinal Chemistry, 56, 5979-83.

[13] Bill, K. L. J., Garnett, J., Meaux. I., Creighton, C. J., Bolshakov, S., Barriere, C. 2016. SAR405838: a novel and potent inhibitor of the MDM2: p53 Axis for the treatment of dedifferentiated liposarcoma. Clinical Cancer Research, 22, 1150-60.

[14] Sun, D., Li, Z., Rew, Y., Gribble, M., Bartberger, M. D., Beck, H. P. 2014. Discovery of AMG 232, a potent, selective, and orally bioavailable MDM2-p53 inhibitor in clinical development. Journal of Medicinal Chemistry, 57, 1454-72.

[15] Holzer, P., Masuya, K., Furet, P., Kallen, J., Valat-Stachyra, T., Ferretti, S., Berghausen. J. 2015. Discovery of a dihydroisoquinolinone derivative (NVP-CGM097): a highly potent and selective MDM2 inhibitor undergoing phase 1 clinical trials in p53wt tumors. Journal of Medicinal Chemistry, 58, 6348-58.

[16] Stachyra-Valat, T., Baysang, F., D'Alessandro, A. C., Dirk, E., Furet, P. 2016. HDM201: biochemical and biophysical profile of a novel highly potent and selective PPI inhibitor of p53-Mdm2. Cancer Research, 76, 1239.

[17] Talevi, A., Bellera, C. L. 2020. Challenges and opportunities with drug repurposing: finding strategies to find alternative uses of therapeutics. Expert Opinion in Drug Discovery, 15(4), 397-401.

[18] Parvathaneni, V., Kulkarni, N. S., Muth, A., Gupta, V. 2019. Drug repurposing: a promising tool to accelerate the drug discovery process. Drug Discovery Today, 24(10), 2076-2085.

[19] Pushpakom, S., Iorio, I., Eyers, P. A., Escott, K. J., Hopper, S., Wells, A., Doig, A. 2019. Drug repurposing: progress, challanges, and recommendations. Nature Reviews Drug Discovery, 18, 41-58.

[20] Tiwari, S., Reuter, N. 2018. Conservation of intrinsic dynamics in proteins-what have computational models taught us. Current Opinion in Structural Biology, 50, 75-81.

[21] Bahar, I., Lezon, T. R., Yang, L. W., Eyal, E. 2010. Global dynamics of proteins: bridging between structure and function. Annual Reviews in Biophysics, 39, 23-42.

[22] Kantarci-Carsibasi, N., Haliloglu, T., Doruker, P. 2008. Conformational transition pathways explored by monte carlo simulations integrated with collective modes. Biophysical Journal, 95 (12), 5862-5873.

[23] Haliloglu, T., Bahar, I., Erman, B. 1997. Gaussian Dynamics of folded proteins, Physical Review Letters, 79, 3090-3093.

[24] Bahar, I., Atilgan, A. R., Demirel, M. C., Erman, B. 1998. Vibrational dynamics of folded proteins: Significance of slow and fast motions in relation to function and stability. Physical Review Letters, 80, 2733-2736.

[25] Atilgan, A. R., Durell, S. R., Jernigan, R. L., Demirel, M. C., Keskin, O., Bahar, I. 2001. Anisotropy of fluctuation dynamics of proteins with an elastic network model. Biophysical Journal, 80, 505-515.

[26] Lu, S. H., Wu, J. W., Liu, H. L., Zhao, J. H. 2011. The discovery of potential acetylcholinesterase inhibitors: a combination of pharmacophore modeling, virtual screening, and molecular docking studies. Journal of Biomedical Science, 18 (1), 8.

[27] Dhanjal, J. K., Sharma, S., Grover, A., Das, A. 2015. Use of ligand-based pharmacophore modeling and docking approach to find novel acetylcholinesterase inhibitors for treating Alzheimer's. Biomedicine Pharmacotherapy, 71, 146-52.

[28] Malik, R., Mehta, P., Srivastava, S., Choudhary, B. S., Sharma, M. 2017. Structure-based screening, ADMET profiling, and molecular dynamic studies on mGlu2 receptor for identification of newer antiepileptic agents. Journal of Biomolecular Structure and Dynamics, 35(16), 3433-3448.

[29] Ece, A. 2020. Towards more effective acetylcholinesterase inhibitors: a comprehensive modelling study based on human acetylcholinesterase protein-drug complex. Journal of Biomolecular Structure and Dynamics, 38 (2), 565-572.

[30] Alamri, M. A., Alamri, M. A. 2019. Pharmacophore and docking-based sequential virtual screening for the identification of novel Sigma 1 receptor ligands. Bioinformation, 15(8), 586-595.

[31] Moussa, N., Hassan, A., Gharaghani, S. 2021. Pharmacophore model, docking, QSAR, and molecular dynamics simulation studies of substituted cyclic imides and herbal medicines as COX-2 inhibitors. Heliyon, 7(4), e06605.

[32] Yuce, M., Cicek, E., Inan, T., Dag, A. B., Kurkcuoglu, O., Sungur, F. A. 2021. Repurposing of FDA-approved drugs against active site and potential allosteric drug-binding sites of COVID-19 main protease. Proteins: Structure Function and Bioinformatics, 89(11), 1425-1441.

[33] Aydin, G. M., Paksoy, N., Orhan, M. D., Avsar, T., Yurtsever, M., Durdagi, S. 2020. Proposing novel MDM2 inhibitors: Combined physics-driven high-throughput virtual screening and in vitro studies. Chemical Biology and Drug Design, 96, 684– 700.

[34] Chen, J., Wang, J., Zhu, W. A. 2013. Computational analysis of binding modes and conformational changes of MDM2 induced by p53 and inhibitor bindings. Journal of Computer Aided Molecular Design, 27, 965-974.

[35] Chene, P. 2004. Inhibition of the p53-MDM2 interaction: targeting a protein-protein interface, Molecular Cancer Research, 2, 20-28.

[36] Das, P., Mattaparthi, V. 2020. Computational investigation on the p53-MDM2 interaction using the potential of mean force study. ACS Omega, 5, 8449-8462.

[37] Dasdidar, S. G., Lane, D. P., Verma, C. S. 2009. Modulation of p53 binding to MDM2: computational studies reveal important roles of Tyr100. BMC Bioinformatics, 10(Suppl 15), S6.

[38] Estrada-Ortiz, N., Neochoritis, C. G., Dömling, A. 2016. How to design a successful p53-MDM2/X interaction inhibitor: a thorough overview based on crystal structures. Chem Med Chem, 1, 757–772.

[39] Atatreh, N., Ghattas, M. A., Bardaweel, S. K., Rawashdeh, S. A., Sorkhy, M. A. 2018. Identification of new inhibitor of MDM2-p53 interactions via pharmacophore and structure-based virtual screening. Drug Design Development and Therapy, 12, 3741-3752.

[40] Pantelopus, G. A., Mukherjee, S., Voelz, V. A. 2015. Microsecond simulations of MDM2 and its complex with p53 yield insight into force field accuracy and conformational Dynamics. Proteins, 83, 1665-1676.

[41] Zhao, P., Cao, H., Chen, Y., Zhu, T. 2019. Insights into the binding mechanisms of inhibitors of MDM2 based on molecular dynamics simulations and binding free energy calculations. Chemical Physics Letters, 728, 94-101.

[42] Chen, J., Wang, J., Zhu, W. A. 2013. Computational analysis of binding modes and conformational changes of MDM2 induced by p53 and inhibitor bindings. Journal of Computer Aided Molecular Design, 27, 965-74.

[43] Zou, R., Zhou, Y., Wang, Y., Kuang, G. 2020. Free Energy Profile and Kinetics of Coupled Folding and Binding of the Intrinsically Disordered Protein p53 with MDM2. Journal of Chemical Information and Modeling, 60(3),1551-1558.

[44] Kantarci-Carsibasi, N. 2021. Elucidation of conformational dynamics of MDM2 and alterations induced upon inhibitor binding using elastic network simulations and molecular docking. Journal of Computational Biophysics and Chemistry, 20 (7), 751-763.

[45] Schrödinger. 2015. Small-molecule drug discovery suite (version 2015-3). New York, NY: Schrödinger, LLC.

[46] Schrödinger. 2018. Maestro (version 2018-4). New York, NY: Schrödinger, LLC.

[47] Sastry, G., Adzhigirey, M., Day, T., Annabhimoju, R., Sherman, W. 2013. Protein and ligand preparation: parameters, protocols, and influence on virtual screening enrichments. Journal of Computer Aided Molecular Design, 27 (3), 221-234.

[48] Jorgensen, W. L., Tirado-Rives, J. 1988. The OPLS (optimized potentials for liquid simulations) potential functions for protein, energy minimizations for crystals of cyclic peptides, and crambin. Journal of American Chemical Society, 118(45), 1657-1666.

[49] Shelly, J. C., Cholleti, A., Frye, L. L., Greenwood, J. R., Timlin, M. R., Uchimaya, M. 2007. Epik: a software program for pK a prediction and protonation state generation for drug-like molecules Journal of Computer Aided Molecular Design, 21 (12), 681-691.

[50] Langer, T., Hoffmann, R., Bachmair, F., Begle, S. 2000. Chemical function based pharmacophore models as suitable filters for virtual screening. Journal of Molecular Structure, 503, 59.

[51] Wolber, G., Langer, T. 2005. LigandScout: 3-D pharmacophores derived from protein-bound ligands and their use as virtual screening filters. Journal of Chemical Informationa and Modeling, 45(1), 160–169.

[52] Halgren, T. A. 1996. Merck molecular force field: Basis, form, scope, parameterization, and performance of MMFF94. Journal of Computational Chemistry, 17 (5–6), 490-519.

[53] Wishart, D. S., Knox, C., Guo, A. C. 2006. Drug Bank: a comprehensive resource for in silico drug discovery and exploration. Nucleic Acids Research, 34, 668-672.

[54] Lipinski, C. A. 2000. Drug-like properties and the causes of poor solubility and poor permeability. Journal of Pharmacology Toxicology Methods, 44(1), 235-249.

[55] Trott, O., Olson, A. J. 2009. AutoDock Vina: Improving the Speed and Accuracy of Docking with a New Scoring Function, Efficient Optimization, and Multithreading. Journal of Computational Chemistry, 31(2), 174-82.

[56] Friesner, R. A., Banks, J. L., Murphy, R. B., Halgren T. A. 2004. Glide: a new approach for rapid, accurate docking and scoring: 1. method and assessment of docking accuracy. Journal of Medicinal Chemistry, 47 (7), 1739-1749.

[57] Friesner, R. A., Murphy, R. B., Repasky, M. P., Frye, L. L., Greenwood, J. R. 2006. Extra precision glide: Docking and scoring incorporating a model of hydrophobic enclosure for protein-ligand complexes. Journal of Medicinal Chemistry, 49 (21), 6177-6196.

[58] Clark, A. J., Tiwary, P., Borrelli, K., Feng, S., Miller, E. B. 2016. Prediction of Protein-Ligand Binding Poses via a Combination of Induced Fit Docking and Metadynamics Simulations. Journal of Chemical Theory and Computation, 12 (6), 2990-2998.

[59] Rastelli, G., Del Rio, A., Degliesposti, G., Sgobba, M. 2010. Fast and accurate predictions of binding free energies using MM-PBSA and MM-GBSA. Journal of Computational Chemistry, 31(4),797-810.

[60] Hou, T., Wang, J., Li, Y., Wang, W. 2011. Assessing the performance of the molecular mechanics/Poisson Boltzmann surface area and molecular mechanics/generalized Born surface area methods. II. The accuracy of ranking poses generated from docking. Journal of Computational Chemistry, 32(5), 866-77.

[61] Jianing, L., Abel, R., Zhu, K., Cao, Y., Zhao, S., Friesner, R. A. 2011. The VSGB 2.0 model: A next generation energy model for high resolution protein structure modeling. Proteins, 79 (10), 2794-2812.

[62] Walter, S. D. 2005. The partial area under the ROC curve. Statistics in Medicine; 24:2025-40.

[63] Basu, S., Wallner, B. 2016. Finding correct protein-protein docking models using PRoQDock. Bioinformatics, 32 (12), i262-i270.

[64] Truchon, J. F., Bayly, C. I. 2007. Evaluating virtual screening methods: good and bad metrics for the "early recognition" problem. Journal of Chemical Information and Modeling, 47(2), 488-508.

[65] Wang, Y., Xiao, J., Suzek, T.O., Zhang, J., Wang, J., Bryant, S. H. 2009. PubChem: a public information system for analyzing bioactivities of small molecules. Nucleic Acids Research, 37, 623–633.

[66] Kim, S., Chen, J., Cheng, T. 2021. PubChem in 2021: new data content and improved web interfaces. Nucleic Acids Research, 49(D1), D1388–D1395.

[67] Overington, J. P., Al-Lazikani, B., Hopkins, A. L. 2006. How many drug targets are there? Nature Reviews Drug Discovery, 5(12), 993-996.

[68] Tetko, I. V., Gasteiger, J., Todeschini, R., Mauri, A. 2005. Virtual computational chemistry laboratory design and description. Journal of Computer Aided Molecular Design, 19, 453-463.

[69] Lee, S. K., Lee, I. H., Kim, H. J., Chang, G. S., Chung, J. E., No, K. T. 2003. The PreADME Approach: web-based program for rapid prediction of physicochemical, drug absorption and drug-like properties. Euro QSAR 2002 designing drugs and crop protectants: processes, problems and solutions, Blackwell Publishing, Massachusetts, USA. 418–420.

Appendix A

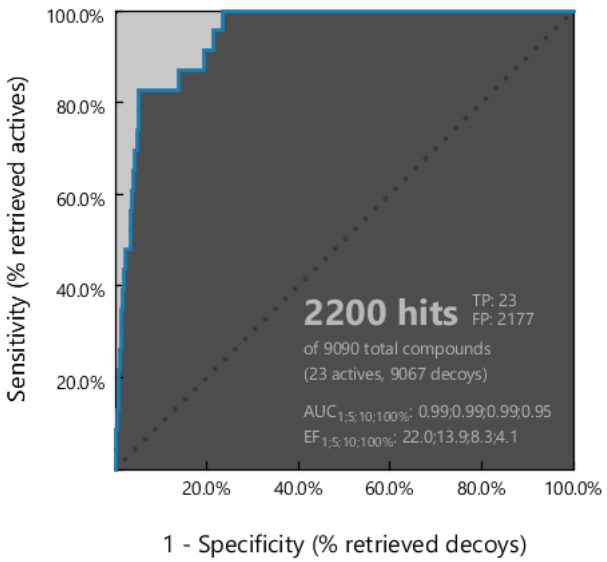

Figure A.1. Receiver operating characteristics (ROC) curve indicating the efficiency of the pharmacophore model used in virtual screening.